

Fine-tuning water exchange on Gd^{III} poly(amino carboxylates) by modulation of steric crowding†

Zoltán Jászberényi, Angélique Sour, Éva Tóth, Meriem Benmelouka and André E. Merbach*

Laboratoire de Chimie Inorganique et Bioinorganique, Ecole Polytechnique Fédérale de Lausanne, ISIC, BCH, CH-1015 Lausanne, Switzerland. E-mail: andre.merbach@epfl.ch; Fax: 41 21 693 9875; Tel: 41 21 693 9871

Received 12th May 2005, Accepted 22nd June 2005

First published as an Advance Article on the web 12th July 2005

In the objective of optimizing water exchange rate on stable, nine-coordinate, monohydrated Gd^{III} poly(amino carboxylate) complexes, we have prepared monopropionate derivatives of DOTA⁴⁻ (DO3A-Nprop⁴⁻) and DTPA⁵⁻ (DTTA-Nprop⁵⁻). A novel ligand, EPTPA-BAA³⁻, the bisamylamide derivative of ethylenepropylenetriamine-pentaacetate (EPTPA⁵⁻) was also synthesized. A variable temperature ¹⁷O NMR study has been performed on their Gd^{III} complexes, which, for [Gd(DTTA-Nprop)(H₂O)]²⁻ and [Gd(EPTPA-BAA)(H₂O)] has been combined with multiple field EPR and NMRD measurements. The water exchange rates, k_{ex}^{298} , are $8.0 \times 10^7 \text{ s}^{-1}$, $6.1 \times 10^7 \text{ s}^{-1}$ and $5.7 \times 10^7 \text{ s}^{-1}$ for [Gd(DTTA-Nprop)(H₂O)]²⁻, [Gd(DO3A-Nprop)(H₂O)]⁻ and [Gd(EPTPA-BAA)(H₂O)]⁻, respectively, all in the narrow optimal range to attain maximum proton relaxivities, provided the other parameters (electronic relaxation and rotation) are also optimized. The substitution of an acetate with a propionate arm in DTPA⁵⁻ or DOTA⁴⁻ induces increased steric compression around the water binding site and thus leads to an accelerated water exchange on the Gd^{III} complex. The k_{ex} values on the propionate complexes are, however, lower than those obtained for [Gd(EPTPA)(H₂O)]²⁻ and [Gd(TRITA)(H₂O)]⁻ which contain one additional CH₂ unit in the amine backbone as compared to the parent [Gd(DTPA)(H₂O)]²⁻ and [Gd(DOTA)(H₂O)]⁻. In addition to their optimal water exchange rate, [Gd(DTTA-Nprop)(H₂O)]²⁻ has, and [Gd(DO3A-Nprop)(H₂O)]⁻ is expected to have sufficient thermodynamic stability. These properties together make them prime candidates for the development of high relaxivity, macromolecular MRI contrast agents.

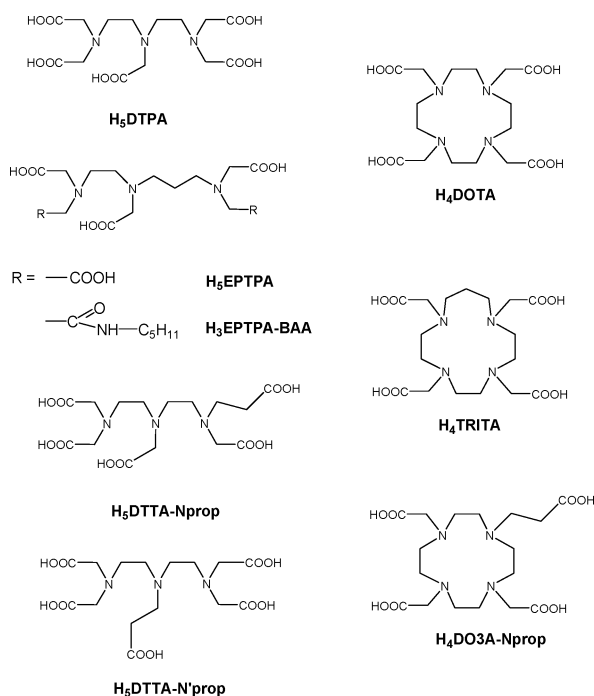
Introduction

Paramagnetic Gd^{III} complexes are extensively applied as contrast agents in Magnetic Resonance Imaging (MRI).¹ By enhancing the intrinsic contrast, they largely contribute to the excellent anatomical resolution of the MR images. Currently emerging applications, such as molecular imaging call for contrast agents of much higher efficiency than the marketed ones. The rational design of high efficacy agents has to consider the relationships between structure, dynamics and the relevant parameters determining relaxation processes. The relaxivity of a contrast agent is defined as the paramagnetic proton relaxation rate enhancement of the bulk water protons, referred to 1 mmolar concentration of gadolinium. The Solomon–Bloembergen–Morgan theory, which relates the observed paramagnetic relaxation rate enhancement to microscopic properties, predicts proton relaxivities over $100 \text{ mM}^{-1} \text{ s}^{-1}$ for Gd^{III} complexes provided the three most important influencing factors, rotation, electron spin relaxation and water exchange are simultaneously optimised.¹ The rotation has to be slowed down which has led in the past few years to the development of macromolecular agents. The optimisation of the electron spin relaxation on Gd^{III} complexes remains a difficult issue, despite the recent theoretical advances.² The optimal value of the water exchange rate, the third determining factor for proton relaxivity, is situated in a relatively small range (around $k_{ex} \approx 5 \times 10^7 \text{ s}^{-1}$). In the currently used Gd^{III}-based contrast agents water exchange is considerably slower ($k_{ex} \approx 1\text{--}4 \times 10^6 \text{ s}^{-1}$).¹ Some bishydrated

Gd^{III} complexes, like TREN-Me-3,2-HOPO derivatives have shown faster water exchange.³ However, for bishydrated chelates a potential drawback is the formation of ternary complexes with small ligands (carbonate, phosphate, citrate) in biological fluids, which can erase any relaxivity gain *in vivo*.⁴

Nine-coordinate, monohydrated Gd^{III} poly(amino carboxylates), including all commercial Gd^{III}-based MRI contrast agents, undergo a dissociative, D, or dissociative interchange, I_d, water exchange, in contrast to the associative, A, mechanism on the eight-coordinate aqua ion, [Gd(H₂O)₈]³⁺.¹ The rate of dissociative exchange processes is primarily determined by the overall charge of the chelate (a more negative charge leads to faster exchange), and by the steric crowding in the inner coordination sphere. An increased steric compression around the inner sphere water molecule will facilitate its leaving which, in a dissociative process, constitutes the rate determining step. Recently we have shown that increased steric compression around the water binding site indeed results in a remarkable acceleration of the water exchange process. Steric compression has been induced in the acyclic DTPA- or the macrocyclic DOTA-type complexes by the insertion of an additional CH₂ group either in the amine backbone of the ligand (EPTPA⁵⁻, TRITA⁴⁻), or in the carboxylate arm (DTTA-N'prop⁵⁻ Scheme 1).^{5,6} While the elongation of the amine backbone results in almost 2 orders of magnitude increase in the water exchange rate of the Gd^{III} complex in comparison to the parent [Gd(DOTA)(H₂O)]⁻ or [Gd(DTPA)(H₂O)]²⁻, the substitution of the central acetate arm by a propionate on the DTPA⁵⁻ ligand gives rise only to a 10-fold increase in k_{ex} . The water exchange rates determined for [Gd(TRITA)(H₂O)]⁻ and [Gd(EPTPA)(H₂O)]²⁻ are slightly higher than the value which would be optimal to attain maximum proton relaxivities. Indeed, when [Gd(EPTPA)(H₂O)]²⁻ was covalently linked to different generations of PAMAM dendrimers, the relaxivity of these macromolecular agents was partially limited by the too fast water exchange of the Gd^{III} chelate.⁷ [Gd(DTTA-N'prop)(H₂O)]²⁻ was found to ensure a

† Electronic supplementary information (ESI) available: Tables of the variable temperature ¹⁷O NMR, EPR and NMRD data. Figures of ¹⁷O NMR experimental data and fitted curves for [Gd(DO3A-Nprop)(H₂O)]⁻, and ¹⁷O NMR, EPR and NMRD experimental data and fitted curves for [Gd(EPTPA-BAA)(H₂O)]⁻. Outline of the Solomon–Bloembergen–Morgan theory used for the analysis of ¹⁷O NMR, EPR and NMRD data. See <http://dx.doi.org/10.1039/b506702b>



Scheme 1

smaller, and more optimal water exchange rate, however, its drawback is the reduced thermodynamic (and very likely kinetic) stability. It was previously reported that the substitution of a terminal acetate of DTPA⁵⁻ by a propionate group (DTTA-Nprop) results in a smaller decrease of the thermodynamic stability for the lanthanide complexes.^{8,9} The monopropionate derivative of the macrocyclic DOTA⁴⁻ ligand can also be expected to form lanthanide complexes of thermodynamic and kinetic stability which is sufficiently high for biomedical applications.

Here we report the characterization of the Gd^{III} complexes formed with the propionate derivatives of DTPA (DTTA-Nprop) and DOTA (DO3A-Nprop) with regard to contrast agent applications. Additionally, the bisamylamide derivative of EPTPA⁵⁻, EPTPA-BAA³⁻ has been synthesized. The replacement of two carboxylates of EPTPA⁵⁻ by amide functions is expected to result in a ~10-fold decrease of k_{ex} on the Gd^{III} complex, as previously proved for amide derivatives of DTPA- and DOTA-type ligands.^{10,11} Based on a variable temperature ¹⁷O NMR study, which was combined with ¹H NMRD and EPR measurements for [Gd(DTTA-Nprop)(H₂O)]²⁻ and [Gd(EPTPA-BAA)(H₂O)]²⁻, we have determined the parameters characterizing water exchange and rotational dynamics on all three Gd^{III} complexes. In the case of the novel EPTPA-BAA³⁻, we have also measured the protonation constants of the ligand and the thermodynamic stability constant for the Gd^{III} complex.

Results and discussion

Experimental

The synthesis of H₅DTTA-Nprop, has been previously reported.¹³ It was carried out in two steps using acidic alkylating arms: reaction of diethylenetriamine with 3-chloropropionic acid first, then with chloroacetate. Each step was followed by long purification by cation exchange chromatography. Here we present a new synthetic procedure involving *t*-butyl esters, which yields products that are easier to purify. The first crucial step is the monoalkylation of diethylenetriamine with *t*-butyl 3-chloropropionate. By silica gel chromatography, we could isolate the compound containing one esterified propionate arm. Further alkylation of the amines with *t*-butyl bromoacetate, followed by hydrolysis of the esters gave the ligand H₅DTTA-Nprop.

The ligand H₃EPTPA-BAA was obtained by conversion of H₅EPTPA¹⁴ into the bis-anhydride¹⁵ followed by reaction with two equivalents of amylamine.

The strategy used to synthesize H₄DO3A-Nprop in the literature¹⁶ was to alkylate DO3A-tris(*t*-butylester) with 3-bromopropionic acid. Our approach, as for H₅DTTA-Nprop, involved *t*-butyl esters. However, purification of the intermediate and the final product was not obvious. We obtained the ligand H₄DO3A-Nprop by repeated additions of *t*-butyl 3-bromopropionate (prepared from 3-bromopropionic acid¹⁷) to commercially available DO3A-tris(*t*-butylester), and followed by hydrolysis of the esters.

Equilibrium studies on H₃EPTPA-BAA

pH-potentiometric titrations have been used to determine the protonation constants of H₃EPTPA-BAA (K_i^H , as defined in eqn. (1)), and the stability constant (K_{ML}) of its Gd³⁺ complex (eqn. (2)).

$$K_i^H = \frac{[H_iL]}{[H_{i-1}][H^+]} \quad i = 0, 1, 2, 3 \text{ and } 4 \quad (1)$$

$$K_{ML} = \frac{[ML]}{[M][L]} \quad (2)$$

The protonation constants of EPTPA-BAA³⁻ as calculated from the titration data (81 data points; Fig. 1) are given in Table 1. For comparison, $\log K_i^H$ values of DTPA⁵⁻, DTTA-Nprop⁵⁻ and EPTPA⁵⁻ are also presented. The protonation sequence has been established by ¹H NMR titrations for analogous ligands like DTPA⁵⁻,¹⁸ DTPA-bis(amides)^{3- 19,20} or EPTPA⁵⁻,²¹ and a similar protonation scheme is expected for the EPTPA-BAA³⁻. The first three protonation steps take place predominantly on the amine nitrogens. The first proton is attached to the central nitrogen, while the second protonation step occurs on a terminal amine, accompanied by the partial transfer of the first proton to the other terminal nitrogen. Then the third proton is probably shared by the central nitrogen and the central carboxylate, as

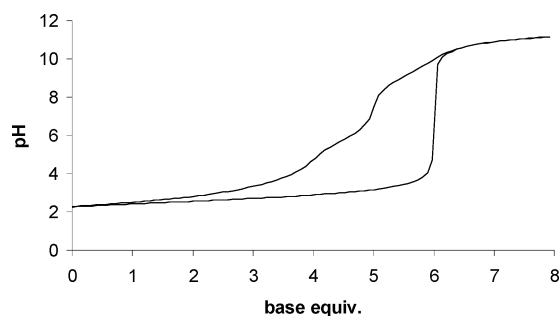


Fig. 1 pH-potentiometric titration curves of the EPTPA-BAA ligand in the absence (left curve) and presence of Gd³⁺ (right curve; Gd³⁺/ligand ratio 1 : 1). $I = 0.1$ M KCl, 25 °C.

Table 1 Protonation constants ($\log K_i^H$) of various ligands and stability constants ($\log K_{ML}$) of their Gd³⁺ complexes (25 °C). The values in parenthesis correspond to one standard deviation

Ligand	DTPA ^a	DTTA-Nprop ^b	EPTPA ^c	EPTPA-BAA ^c
L + H ⁺	10.41	9.64	10.60	9.08 (0.05)
LH + H ⁺	8.37	8.86	8.92	5.76 (0.07)
LH ₂ + H ⁺	4.09	4.52	5.12	3.57 (0.08)
LH ₃ + H ⁺	2.51	3.54	2.80	2.22 (0.08)
LH ₄ + H ⁺	2.04	2.79		
Gd ³⁺ + L	22.50	19.74	17.5 ^d	13.44(0.03)
GdL + H ⁺	1.80	3.74		

^a Ref. 12 $I = 0.1$ M (CH₃)₄NCl. ^b Ref. 8 $I = 0.1$ M KNO₃. ^c Ref. 21 $I = 0.1$ M (CH₃)₄NNO₃. ^d Ref. 6 $I = 0.1$ M (CH₃)₄NCl. ^e This work $I = 0.1$ M KCl.

in DTPA-bis(amide) derivatives. In comparison to DTPA⁵⁻, DTTA-N-prop⁵⁻ and EPTPA⁵⁻, all protonation constants of EPTPA-BAA³⁻ are significantly lower. This decrease in logK₁^H brought by the replacement of two carboxylates by amide groups may result from the formation of hydrogen bonds between amide hydrogens and amine nitrogens or carboxylate oxygens.^{19,20}

The stability constant of Gd(EPTPA-BAA) was determined by direct pH-potentiometry (from 50 data points at pH 1.9–4.8). The titration curve in the presence of Gd³⁺ is shown in Fig. 1; the stability constant is given in Table 1. The formation of protonated [GdH(EPTPA-BAA)(H₂O)]⁺ complex could not be detected. Among the selection of ligands listed in Table 1, which all similarly contain oxygen and nitrogen donor atoms, EPTPA-BAA³⁻ forms the least stable complex with Gd³⁺. Due to the propylene bridge between two amine nitrogens, EPTPA-type complexes all contain one six-membered chelate ring, less stable than a five-membered ring. This is the reason why EPTPA-derivatives form lower stability complexes with metal ions than the DTPA-analogues.⁶ In addition, the replacement of two carboxylates with amide groups further destabilizes the complex, as a consequence of the lower negative charge and reduced amine basicity of amide derivatives.

¹⁷O NMR, EPR and NMRD measurements

The water exchange rate was determined for the Gd^{III} complexes of the ligands DTTA-Nprop⁵⁻, DO3A-Nprop and EPTPA-BAA³⁻ from a variable temperature ¹⁷O NMR study. Additionally, variable temperature EPR spectra were recorded and proton relaxation rates measured on aqueous solutions of [Gd(EPTPA-BAA)(H₂O)] and [Gd(DTTA-Nprop)(H₂O)]²⁻ with the objective of assessing all parameters that describe water exchange, rotation, electronic relaxation and proton relaxivity. All available experimental data for a given Gd^{III} complex, *i.e.* the oxygen-17 chemical shifts ($\Delta\omega_i$), longitudinal ($1/T_{1r}$) and transverse ($1/T_{2r}$) relaxation rates, the electronic relaxation rates ($1/T_{2e}$) and the longitudinal proton relaxivities (r_1 , when measured) were analysed simultaneously. The ¹⁷O NMR data on [Gd(DO3A-Nprop)(H₂O)]⁻ were fitted to the Solomon–Bloembergen–Morgan equations.¹ For the two other complexes, where we had variable field EPR and variable temperature NMRD data in addition to the ¹⁷O relaxation rates and chemical shifts, the electronic relaxation has been described by the Rast–Borel theory, involving both transient and static zero-field-splitting contributions.^{2,22} Equations used in the fit can be found in the ESI†.

For all three Gd^{III} complexes we assumed one inner sphere water molecule ($q = 1$). This is based (i) on the analogy to previously studied, DTPA- or DOTA-type Gd^{III}-chelates where the ligand possesses eight donor atoms, and (ii) on the experimental ¹⁷O chemical shifts, which are proportional to the

Gd^{III} concentration and to q (the value of the scalar coupling constant, A/\hbar , does not change much within the family of similar Gd^{III} complexes). In the analysis of the ¹⁷O NMR, EPR and NMRD data, some of the parameters were fixed to common and physically meaningful values. For the distances we used $r_{\text{GdO}} = 2.5 \text{ \AA}$ (Gd electron spin and ¹⁷O nucleus distance), $r_{\text{GdH}} = 3.1 \text{ \AA}$ (Gd electron spin and ¹H nucleus distance) and $a_{\text{GdH}} = 3.5 \text{ \AA}$ (closest approach of the bulk water protons). The longitudinal ¹⁷O relaxation is related to motions of the Gd-coordinated water oxygen vector, while the proton relaxation is determined by motions of the Gd-coordinated water proton vector. For the ratio of the rotational correlation time of the Gd–H_{water} and Gd–O_{water} vectors, $\tau_{\text{RH}}/\tau_{\text{RO}}$, similar values have been found for various small molecular weight, monohydrated Gd^{III} complexes, both by experimental studies and MD simulations ($\tau_{\text{RH}}/\tau_{\text{RO}} = 0.65 \pm 0.2$).²⁵ This $\tau_{\text{RH}}/\tau_{\text{RO}}$ ratio, within the given error, is considered as a common value for the ratio of the two rotational correlation times. In the simultaneous analysis of ¹⁷O NMR, EPR and NMRD data for the [Gd(DTTA-Nprop)(H₂O)]²⁻ and [Gd(EPTPA-BAA)(H₂O)] complexes, we fixed the $\tau_{\text{RH}}/\tau_{\text{RO}}$ ratio to 0.65. The quadrupolar coupling constant for the bound water oxygen, $\chi(1 + \eta^2/3)^{1/2}$, was fitted and a value of 10.9 ± 2.5 and 7.3 ± 1.6 MHz was found for [Gd(DTTA-Nprop)(H₂O)]²⁻ and [Gd(EPTPA-BAA)(H₂O)], respectively. The empirical constant C_{os} that characterizes the outer sphere contribution to the ¹⁷O chemical shift, was fixed for all three Gd^{III} complexes studied to 0.1. Proton relaxivities only above 5 MHz were included in the fit, within the validity of the Redfield relaxation theory. The limits of the Redfield theory have been previously discussed.² The experimental ¹⁷O NMR, EPR and NMRD data and the fitted curves for [Gd(DTTA-Nprop)(H₂O)]²⁻ are presented in Fig. 2; for the two other complexes the figures can be found in the ESI†. The most relevant parameters obtained in the fit are shown in Tables 2 and 3. The diffusion constant, D_{GdH}^{298} , and its activation

Table 3 Parameters obtained from the fitting of ¹⁷O NMR data for macrocyclic Gd^{III} complexes

Ligand	DOTA ^a	DO3A-Nprop ^b	TRITA ^c
$k_{\text{ex}}^{298} / 10^7 \text{ s}^{-1}$	0.46	6.1 ± 1.9	270
$\Delta H^\ddagger / \text{kJ mol}^{-1}$	54.5	39.2 ± 3.4	17.5
$\Delta S^\ddagger / \text{J mol}^{-1} \text{ K}^{-1}$	+65	$+35.6 \pm 5.7$	-24
$A/\hbar / 10^6 \text{ rad s}^{-1}$	-4.0	-3.3 ± 0.5	-3.8
$\tau_{\text{RO}}^{298} / \text{ps}$	100	153 ± 12	82
$E_{\text{R}} / \text{kJ mol}^{-1}$	20	22.4 ± 6.1	21.9
$\tau_{\text{v}}^{298} / \text{ps}$	0.65	7.0	^d
$E_{\text{v}} / \text{kJ mol}^{-1}$	8.6	1.0	^d
$\Delta^2 / 10^{20} \text{ s}^{-2}$	—	0.97 ± 0.08	^d

^a Ref. 23. ^b From ¹⁷O NMR, NMRD and EPR data. ^c Present work. ^d Ref. 5. ^e Not obtained. Underlined parameters were fixed in the fit.

Table 2 Parameters obtained from the simultaneous fitting of ¹⁷O NMR, NMRD and EPR data for various acyclic Gd^{III} complexes

Ligand	DTPA ^a	DTPA-BMA ^b	DTTA-N'prop ^c	DTTA-Nprop ^d	EPTPA ^e	EPTPA-BAA ^d
$k_{\text{ex}}^{298} / 10^7 \text{ s}^{-1}$	0.38	0.043	3.1	8.0 ± 1.5	33	5.7 ± 0.8
$\Delta H^\ddagger / \text{kJ mol}^{-1}$	52.9	46.6	30.8	19.5 ± 3.0	27.9	28.2 ± 3.7
$\Delta S^\ddagger / \text{J mol}^{-1} \text{ K}^{-1}$	+54	+18.9	+2.0	-28.2 ± 5.1	+11.0	-2.2 ± 6.0
$A/\hbar / 10^6 \text{ rad s}^{-1}$	-3.9	-3.6	-3.3	-3.4 ± 0.3	-3.9	-3.5 ± 0.8
$\tau_{\text{RO}}^{298} / \text{ps}$	115	167	121	107 ± 16	75	192 ± 18
$E_{\text{R}} / \text{kJ mol}^{-1}$	20	21.6	17.4	20.0 ± 4.2	17.7	19.0 ± 5.9
$\tau_{\text{v}}^{298} / \text{ps}$	0.10	34	18	7.7 ± 0.5	22.4	4.0 ± 0.3
$E_{\text{v}} / \text{kJ mol}^{-1}$	1.0	9	1	0.8 ± 0.3	1	1
$\Delta^2 / 10^{20} \text{ s}^{-2}$	—	0.38	1.2	—	0.76	—
g	1.99	—	—	1.99 ± 0.01	—	1.99 ± 0.02
$a_2 / 10^{10} \text{ s}^{-1}$	0	—	—	0.51 ± 0.02	—	0.39 ± 0.03
$a_4 / 10^{10} \text{ s}^{-1}$	0.016	—	—	0	—	0
$a_6 / 10^{10} \text{ s}^{-1}$	0.0280	—	—	0	—	0
$a_{2T} / 10^{10} \text{ s}^{-1}$	0.48	—	—	0.48 ± 0.01	—	0.38 ± 0.01

^a Ref. 23. ^b Ref. 24. ^c Ref. 6, only from ¹⁷O NMR. ^d Present work. ^e Ref. 6 from ¹⁷O NMR and EPR data. Underlined values were fixed in the fit.

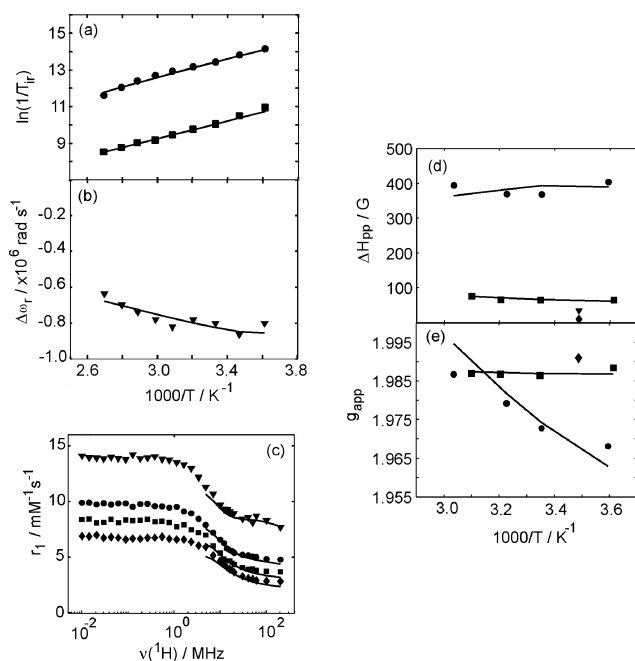


Fig. 2 Temperature dependence of reduced ^{17}O transverse (●), longitudinal (■) relaxation rates (a), reduced chemical shifts (b) at 9.4 T; proton relaxivities at 5.1 °C (▼), 25.0 °C (●), 37.1 °C (■) and 49.7 °C (◆) (c); EPR peak-to-peak line widths (d) and the apparent g -factor (e) at 9.4 GHz (●), 35 GHz (■) and 94 GHz (only one point: ▼-measured, ◆-calculated) for $[\text{Gd}(\text{DTTA-Nprop})(\text{H}_2\text{O})]^{2-}$. The curves represent the fit to the experimental data points.

energy, E_{DGdH} , were calculated to be $(19 \pm 2) \times 10^{-10} \text{ m}^2 \text{ s}^{-1}$, $(20 \pm 2) \times 10^{-10} \text{ m}^2 \text{ s}^{-1}$ and $(23 \pm 1) \text{ kJ mol}^{-1}$, $(30 \pm 3) \text{ kJ mol}^{-1}$ for $[\text{Gd}(\text{DTTA-Nprop})(\text{H}_2\text{O})]^{2-}$ and $[\text{Gd}(\text{EPTPA-BAA})(\text{H}_2\text{O})]$, respectively.

The values of the rotational correlation time obtained from the ^{17}O longitudinal relaxation rates for $[\text{Gd}(\text{DO3A-Nprop})(\text{H}_2\text{O})]^-$ and from the ^{17}O and ^1H longitudinal relaxation rates for $[\text{Gd}(\text{DTTA-Nprop})(\text{H}_2\text{O})]^{2-}$ and $[\text{Gd}(\text{EPTPA-BAA})(\text{H}_2\text{O})]$ are in the usual range expected for small molecular weight chelates. The τ_{RO}^{298} calculated for the bisamylamide $[\text{Gd}(\text{EPTPA-BAA})(\text{H}_2\text{O})]$ complex is only slightly higher than that of $[\text{Gd}(\text{DTPA-BMA})(\text{H}_2\text{O})]$ which shows that—as expected—the five-carbon chain is still too short to promote micellar aggregation in aqueous solution that would considerably slow down the rotational motion.

It has to be noted that all three Gd^{III} complexes studied here present “intermediate” water exchange rates. This means that the slow exchange regime is not visible in the $\ln(1/T_{2r})$ vs. $1000/T$ curves, on the other hand, we are far from the “very fast” exchange, where the electron spin relaxation has negligible contribution to the experimentally measured ^{17}O transverse relaxation rates. For a Gd^{III} complex with slow water exchange, at low temperatures the reduced transverse ^{17}O relaxation rates, $1/T_{2r}$, increase with increasing temperature (slow exchange regime). Under such conditions, $1/T_{2r}$ is determined exclusively by the water exchange rate, and electronic relaxation does not contribute to the experimental ^{17}O relaxation rates. Therefore, even in the lack of EPR data, k_{ex} can be determined with high exactitude. On the other hand, the reduced transverse ^{17}O relaxation rates can also decrease with increasing temperature (fast exchange regime). Here they are influenced by the relaxation rate of the coordinated water oxygen, $1/T_{2m}$. $1/T_{2m}$ is determined by both the rate of water exchange and the rate of electron spin relaxation. The faster the water exchange, the less influence the electron spin relaxation has. In the situation of a “very fast” water exchange, electron spin relaxation has no, or only a negligible role in determining the experimentally measured ^{17}O $1/T_{2r}$ rates, as was typically the case for $\text{Eu}(\text{H}_2\text{O})_7^{2+}$ ($k_{\text{ex}}^{298} = 5.0 \times 10^9 \text{ s}^{-1}$)²⁶ or $[\text{Gd}(\text{EPTPA})(\text{H}_2\text{O})]^{2-}$ ($k_{\text{ex}}^{298} = 3.3 \times 10^9 \text{ s}^{-1}$;

contribution of $1/T_{1e}$ to $1/T_{2m}$ was 6% maximum).⁶ For an intermediate water exchange rate, however, the contribution of the electron spin relaxation to the observed transverse relaxation rate in ^{17}O NMR can be important, therefore independent information from EPR is very helpful in determining exact water exchange rates. It is also well-known that the traditional Solomon–Bloembergen–Morgan theory has serious limitations in describing the magnetic field dependence of the electron spin relaxation rates. Therefore, it is particularly important that in the case of $[\text{Gd}(\text{DTTA-Nprop})(\text{H}_2\text{O})]^{2-}$ and $[\text{Gd}(\text{EPTPA-BAA})(\text{H}_2\text{O})]$ which both present intermediate water exchange rates, we had independent information on electronic relaxation from EPR data, and the combined analysis of EPR and ^{17}O NMR (and NMRD) was performed by using an adequate theory of electronic relaxation, capable of describing field dependences in a large domain (the EPR data were obtained at $B = 0.34 \text{ T}$ (X-band), 1.25 T (Q-band) and 3.41 T (W-band), whereas the ^{17}O NMR was performed at 9.4 T). On the other hand, the water exchange rate on $[\text{Gd}(\text{DO3A-Nprop})(\text{H}_2\text{O})]^-$ was calculated only from ^{17}O NMR data. Consequently, the realistic, physically meaningful error on it is clearly higher; one can estimate it to be $\sim \pm 50\%$, in contrast to the statistical error of the fit as given in Table 3.

Water exchange

Tables 2 and 3 summarize water exchange parameters for a selection of MRI-related, linear (DTPA-type) and macrocyclic (DOTA-type) Gd^{III} complexes. Despite the structural similarity of the ligands, the water exchange rates on their Gd^{III} complexes cover three orders of magnitude from the DTPA-bisamide to EPTPA⁵⁻. The origin of this remarkable variation is the differing steric compression that the ligand induces around the water binding site. By varying the distance between the donor atoms that coordinate to the metal, one can tune the steric crowding in the inner coordination sphere.²⁷ All these nine-coordinate Gd^{III} complexes undergo a dissociatively activated water exchange, for which steric crowding is of primary importance. The leaving of the coordinated water molecule, which is the rate-determining step, is largely facilitated by an increased steric crowding.

Unfortunately, when one ethylene is replaced by a propylene bridge in the amine skeleton of the ligand, the thermodynamic and kinetic stability of the complex is reduced. Moreover, the water exchange rate on $[\text{Gd}(\text{EPTPA})(\text{H}_2\text{O})]^{2-}$ and $[\text{Gd}(\text{TRITA})(\text{H}_2\text{O})]^-$ already exceeds the optimal value. Both problems can be resolved if the steric compression is introduced by elongation of a carboxylate arm. $[\text{Gd}(\text{DTTA-Nprop})(\text{H}_2\text{O})]^{2-}$ and $[\text{Gd}(\text{DO3A-Nprop})(\text{H}_2\text{O})]^-$ have intermediate water exchange rates, which fall exactly in the optimal range. It is interesting to observe in the DTPA-family that the position of the propionate arm also has an influence on the water exchange rate; the complex with the terminal propionate exchanges its inner sphere water 2.6 times faster than the analogous chelate with a central propionate. This structural difference also has a significant consequence on the thermodynamic stability of the Gd^{III} complex: for the central propionate the stability constant is three orders of magnitude lower than that for the terminal propionate ($\log K_{\text{GdL}} = 16.7$ vs. 19.7).^{8,9}

The thermodynamic stability constant has not been reported for $[\text{Gd}(\text{DO3A-Nprop})(\text{H}_2\text{O})]^-$, however, we can expect that it is higher than $\log K_{\text{GdL}} = 19.17$ for $[\text{Gd}(\text{TRITA})(\text{H}_2\text{O})]^-$.²⁸ The substitution of an acetate with a propionate arm in $[\text{Gd}(\text{DTPA})(\text{H}_2\text{O})]^{2-}$ decreases the stability constant of the complex by 2.7 logK units (Table 1), thus for $[\text{Gd}(\text{DO3A-Nprop})(\text{H}_2\text{O})]^-$ one can expect $\log K_{\text{GdL}} \approx 22$ ($\log K_{\text{GdDOTA}} = 24.7$).²⁹ Beside the thermodynamic stability, kinetic inertness is also very important for biomedical applications of metal complexes. No data are available for the linear $[\text{Gd}(\text{EPTPA})(\text{H}_2\text{O})]^{2-}$. For $[\text{Gd}(\text{TRITA})(\text{H}_2\text{O})]^-$, it has been recently proved that

the kinetic inertness, characterized by the dissociation half-life of the Gd^{III} complex, is three orders of magnitude lower than for [Gd(DOTA)(H₂O)]⁻³⁰ (though still higher than for [Gd(DTPA)(H₂O)]²⁻, the most widely used MRI contrast agent). Similarly to the thermodynamic stability, we can assume a higher kinetic inertness for the propionate complexes [Gd(DTTA-Nprop)(H₂O)]²⁻ and more particularly [Gd(DO3A-Nprop)(H₂O)]⁻ as compared to [Gd(EPTPA)(H₂O)]²⁻ or [Gd(TRITA)(H₂O)]⁻, and this kinetic inertness would certainly fulfil the requirements of safe *in vivo* application.

The water exchange rate on [Gd(EPTPA-BAA)(H₂O)] is one order of magnitude lower than that on [Gd(EPTPA)(H₂O)]²⁻. A decrease in *k*_{ex} has been previously observed for all amide derivatives with respect to the carboxylate parent complexes. The magnitude of this decrease on replacing one carboxylate by an amide function was found to be little dependent of the ligand structure: it was a factor of 3–4 per each carboxylate replaced in both DTPA- or DOTA-type ligands. Thus the value of 5.7 × 10⁷ s⁻¹ for [Gd(EPTPA-BAA)(H₂O)] as compared to 33 × 10⁷ s⁻¹ for [Gd(EPTPA)(H₂O)]²⁻ follows well this empirical observation.

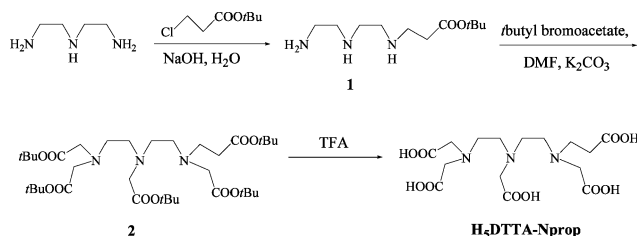
In conclusion, we have demonstrated that by minor, appropriate changes in the ligand structure one can fine-tune the steric compression around the water binding site in nine-coordinate, monohydrated Gd^{III} poly(amino carboxylate) complexes, which translates to the fine-tuning of the rate of water exchange. The introduction of one six-membered chelate ring in the complex always gives rise to an increased steric crowding. The steric crowding and the consequent acceleration of the water exchange is more important on the elongation of the amine backbone (EPTPA⁵⁻, TRITA⁴⁻) than on the elongation of the carboxylate pending arm (DTTA-Nprop⁵⁻, DO3A-Nprop⁴⁻). For the propionate derivative ligands DTTA-Nprop⁵⁻, DO3A-Nprop⁴⁻ we observe a moderate, (optimal) water exchange rate. This, together with the limited reduction of the stability of the Gd^{III} complexes makes the ligands DTTA-Nprop⁵⁻ and DO3A-Nprop⁴⁻ prime candidates for the development of high-relaxivity, macromolecular MRI contrast agents.

Experimental

The synthetic procedures of compounds H₂DTTA-Nprop, H₃EPTPA-BAA and H₄DO3A-Nprop are summarized in Schemes 2, 3 and 4. Commercially available chemicals were reagent grade and were used without further purification. *t*-Butyl 3-chloropropionate was synthesized according to a published procedure.³¹ H₃EPTPA was obtained following the literature.¹⁴ DO3A tris(*t*-butylester) was purchased from Macrocyclics.

Synthesis of the ligands

H₂DTTA-Nprop



Scheme 2

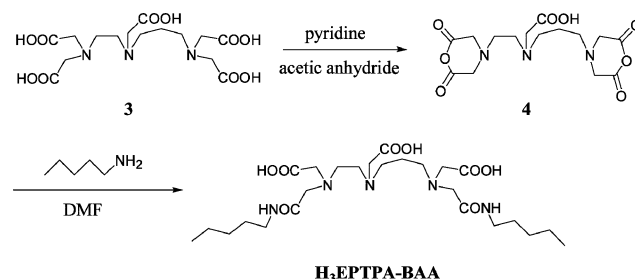
Synthesis of compound 1. *t*-Butyl 3-chloropropionate (2 g, 12.15 mmol) was added to a refluxing solution of diethylene triamine (3.9 ml, 36.29 mmol) and NaOH (0.486 mg, 12.15 mmol) in water (3.6 ml) and reflux was continued for 25 min. After cooling, the resulting yellow solution was extracted with CH₂Cl₂ (10 ml). Purification by silica gel chromatography

using CH₂Cl₂/MeOH/NH₃ (50 : 25 : 5) as eluent afforded 0.72 g (26%) of compound 1. δ_H/ppm (400 MHz, CDCl₃) 2.94 (t, *J* 6.5 Hz, 2H), 2.90 (t, *J* 5.7 Hz, 2H), 2.83 (s, 4H), 2.78 (t, *J* 5.9 Hz, 2H), 2.52 (t, *J* 6.5 Hz, 2H), 1.54 (s, 9H); δ_C/ppm (400 MHz, CDCl₃) 172.4, 80.6, 52.6, 49.3, 45.3, 41.9, 36.0, 28.3.

Synthesis of compound 2. To a solution of 1 (0.55 g, 2.38 mmol) in DMF (12 ml) was added *t*-butyl bromoacetate (1.92 g, 9.88 mmol) and K₂CO₃ (1.38 g, 10.0 mmol) and the resulting mixture was stirred overnight at room temperature. After filtration and evaporation of the solvent, the crude product was extracted with H₂O (9 ml) and CHCl₃ (16 ml). The organic phase was dried with Na₂SO₄ and evaporated to dryness. Purification through a silica gel column using EtOAc/heptane (1/1) as eluent afforded 1.3 g of compound 2 (yield 80%). *m/z* (MS-ESI) 689 [M + H]⁺; δ_H/ppm (400 MHz, CDCl₃) 3.43 (4H, s), 3.32 (2H, s), 3.26 (2H, s), 2.89 (2H, dd, *J* 7.2 Hz, *J* 7.5 Hz), 2.77 (4H, m), 2.70 (4H, s), 2.34 (2H, dd, *J* 7.2 Hz, *J* 7.5 Hz), 1.43 (36H, s), 1.41 (9H, s); δ_C/ppm (400 MHz, CDCl₃) 172.0, 171.1, 170.9, 170.8, 81.0, 80.8, 80.3, 56.3, 56.0, 53.2, 53.0, 52.6, 52.5, 50.5, 34.8, 28.3, 28.2.

Synthesis of H₂DTTA-Nprop. A solution of 2 (1.27 g, 1.86 mmol) in TFA (20 ml) was stirred at room temperature for 18 h. The light yellow solution was filtered and evaporated to dryness. The residue was dissolved in water (50 ml) and evaporated. This operation was repeated twice. Et₂O (50 ml) was added and then evaporated. This operation was also repeated twice. A beige powder was obtained (1.0 g, 92%). (Found: C, 36.80; H, 4.65; N, 6.78; F, 14.22. Calc. For C₁₅H₂₅N₃O₁₀(CF₃COOH)_{1.5}(H₂O)_{0.5}: C, 36.80; H, 4.72; N, 7.15; F, 14.55%); *m/z* (MS-ESI) 408 [M + H]⁺; δ_H/ppm (400 MHz, D₂O) 3.12 (2H, t, *J* 6.9 Hz), 3.35 (2H, t, *J* 6.1 Hz), 3.40 (2H, t, *J* 6.6 Hz), 3.67–3.72 (4H, m), 3.479–3.82 (4H, m), 4.27 (2H, s), 4.30 (4H, s). δ_C/ppm (400 MHz, D₂O) 174.3, 173.9, 169.3, 168.7, 55.5, 54.5, 53.9, 53.5, 52.7, 50.9, 49.7, 49.0, 28.3.

H₃EPTPA-BAA



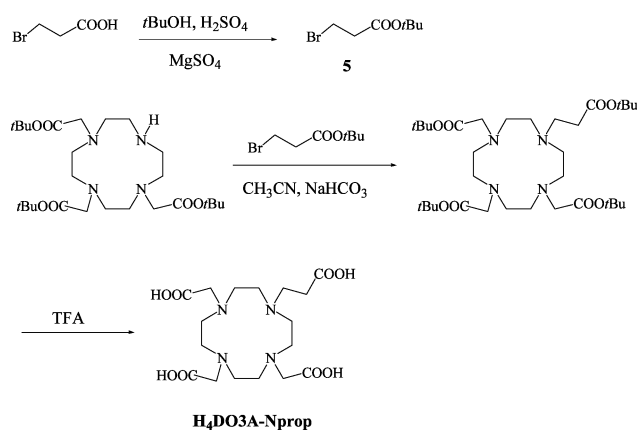
Scheme 3

Synthesis of compound 4. To a suspension of H₃EPTPA 3 (1.344 g, 3.30 mmol) in pyridine (2 ml) was added acetic anhydride in three portions (2.9 ml, 30.88 mmol). The starting compound dissolved progressively. The solution was heated at 50 °C for 1 h then stirred at room temperature for 3 h. Et₂O (30 ml) was added, the precipitate was washed with Et₂O and dried under vacuum to afford a white and yellow crispy solid 4 which was used without further purification.

Synthesis of H₃EPTPA-BAA. To a solution of EPTPA-bis(anhydride) 4 (1.22 g, 3.30 mmol) in DMF (50 ml) was added amylamine (0.75 ml, 6.60 mmol) in three portions. The mixture was stirred for 1 h at 40 °C. After cooling, the solvent was evaporated. The resulting yellow oil was dissolved in H₂O (15 ml) and Et₂O (15 ml). This operation was repeated twice. The resulting yellow powder was dissolved in hot EtOH (80 ml) and heptane (5 ml) was added. A white powder precipitated during cooling, it was collected by filtration, washed with Et₂O and dried *in vacuo* affording 0.99 g (global yield 55%) of H₃EPTPA-BAA as a white powder. (Found: C, 54.57; H, 8.82; N, 12.67; O,

22.82. Calc. For C₂₅H₄₇N₅O₈(H₂O)_{0.25}: C, 54.57; H, 8.70; N, 12.73; F, 23.99%; δ_{H} /ppm (400 MHz, D₂O) 4.14 (2H, s), 3.90 (2H, s), 3.83 (2H, s), 3.53 (2H, s), 3.51 (2H, s), 3.44–3.35 (6H, m), 3.28–3.24 (4H, m), 3.18–3.16 (2H, m), 2.24 (m, 2H), 1.56–1.49 (4H, m), 1.32–1.26 (m, 8H), 0.90–0.86 (6H, m). δ_{C} /ppm (400 MHz, D₂O) 175.5, 171.5, 170.4, 169.9, 165.2, 58.4, 57.2, 56.7, 55.9, 55.7, 53.6, 53.4, 52.8, 50.8, 39.8, 39.4, 28.5, 28.4, 28.2, 27.9, 26.5, 21.8, 21.7, 19.7, 13.4, 13.3.

H₄DO3A-Nprop



Scheme 4

Synthesis of compound 5. H₂SO₄ (0.92 ml, 16.34 mmol) was added to a stirred suspension of anhydrous MgSO₄ (7.87 g, 65.36 mmol) in CH₂Cl₂ (20 ml) under argon. The resulting suspension was stirred for 15 min then 3-bromopropionic acid (2.5 g, 16.34 mmol) and *t*-BuOH (7.48 ml, 81.70 mmol) were added. The mixture was stirred at room temperature for 18 h. A saturated aqueous solution of NaHCO₃ (100 ml) was slowly added and the mixture was stirred until dissolution of MgSO₄. The product was extracted with CH₂Cl₂ (2 × 50 ml). The organic phase was washed with H₂O (40 ml), dried with MgSO₄ and evaporated to dryness. A colorless liquid **5** was obtained (1.2 g, 35%). δ_{H} /ppm (400 MHz, CDCl₃) 3.54 (2H, t, *J* 13.7 Hz), 2.81 (2H, t, *J* 13.7 Hz), 1.46 (9H, s).

Synthesis of H₄DO3A-Nprop. To a solution of DO3A tris(*t*-butylester) (180 mg, 0.35 mmol) in acetonitrile (3.5 ml) was added Cs₂CO₃ (285 mg, 0.87 mmol) and **5** (73.2 mg, 0.35 mmol) under argon. The resulting suspension was heated at 60 °C for 2 days. After evaporation of the solvent, the crude product was dissolved in water (10 ml) and extracted with CH₂Cl₂ (3 × 10 ml). The organic phase was dried with MgSO₄ and evaporated to dryness. The ES-MS spectra showed the presence of a small pic of the desired compound. The reaction and the work-up were repeated twice (with addition of **5**). The mass spectra showed that the pic of the final compound was higher than the starting material and revealed also the presence of secondary products. A SiO₂ chromatography eluted with CH₂Cl₂/MeOH (9/1) allowed us to obtain 94 mg of the tetra ester in the presence only of the starting material. This mixture was not purified further and used for the next step. It was dissolved in trifluoroacetic acid (10 ml) and stirred at room temperature for 24 h. After evaporation to dryness the compound was redissolved in water (12 ml) and evaporated. This operation was repeated twice. Et₂O (12 ml) was then added. Evaporation to dryness gave a yellow powder which was dissolved in a minimum of water and loaded onto a cation-exchange chromatography column (Bio-Rad AG 50W-X4, H⁺ form, 6 ml). The column was washed with water until the pH of the eluate was neutral and the product mixture was eluted in one fraction with NH₃ (0.5 M, 50 ml). This fraction was evaporated to dryness, dissolved in water (2 ml) and NaOH 1 M was added until the pH reached 12. This solution was loaded onto an

anion-exchange chromatography column (Bio-Rad AG 1-X4, converted into HCOO⁻ form, 6 ml). The column was washed with water until the pH of the eluate was neutral and the product was eluted with a 0.1–0.3 M gradient of HCOOH (total volume of gradient ≈ 80 ml). The fractions containing the product were evaporated and the anion-exchange chromatography was repeated twice until the product could be isolated. After removal of the solvents and drying under reduced pressure, H₄DO3A-Nprop was obtained as a white powder (20 mg, 14%). *m/z* (MS-ESI) 419 [M + H]⁺.

Preparation of the stock solutions

The stock solution of Gd(ClO₄)₃ was prepared by dissolving Gd₂O₃ in a slight excess of HClO₄ (Merck p.a. 60%) in double distilled water. Its concentration was determined by complexometric titration with standardized Na₂H₂EDTA solution using xylenol orange as indicator (H₄edta = ethylenediaminetetraacetic acid). The solutions of the GdL complexes were prepared by mixing equimolar amounts of Gd(ClO₄)₃ and the ligand. A slight ligand excess (5%) was used and the pH was adjusted to about 5–5.5 by adding 0.1 M HClO₄ or 0.1 M NaOH. The absence of free metal was checked in each sample by the xylenol orange test.

In the ¹⁷O NMR samples, ¹⁷O enriched water (Izotec, ¹⁷O: 11.4%) was used (final enrichment ~1–2%) to improve sensitivity and the pH was checked again. The concentration and pH of the samples were the following: [Gd(DTTA-Nprop)(H₂O)]²⁻: 4.510 × 10⁻² mol kg⁻¹, pH = 5.4 (¹⁷O NMR), 9.931 × 10⁻³ M, pH = 5.6 (NMRD), 4.942 × 10⁻² M, pH = 5.3 (EPR); [Gd(EPTPA-BAA)(H₂O)]: 3.870 × 10⁻² mol kg⁻¹, pH = 5.5 (¹⁷O NMR), 1.017 × 10⁻² M, pH = 5.6 (NMRD), 4.348 × 10⁻² M, pH = 5.5 (EPR); [Gd(DO3A-Nprop)(H₂O)]⁻: 2.420 × 10⁻² mol kg⁻¹, pH = 5.8 (¹⁷O NMR).

Equilibrium measurements

The protonation constants of EPTPA-BAA³⁻ and the stability constant with Gd³⁺ were determined by pH-potentiometric titration at 25 °C in 0.1 M KCl. A Metrohm Dosimat 665 automatic burette, a combined glass electrode (C14/02-SC, reference electrode Ag/AgCl in 3 M KCl, Møeller Scientific Glass Instruments, Switzerland) and a Metrohm 692 pH/ion-meter were used for the titrations. The samples (3 ml) were stirred and N₂ was bubbled through the solutions.

The concentration of EPTPA-BAA³⁻ (2 mM) was determined using the titration curves obtained in the presence and absence of an excess of CaCl₂ (*c*_{Ca}/*c*_L ≈ 40, when all the dissociable protons of the ligand dissociate).

Protonation constants were determined in 2 mM EPTPA-BAA³⁻ solutions titrated with standardized KOH solution (0.05 M). In the EPTPA-BAA-Gd³⁺ system, the ligand and metal concentrations were both 2 mM. The H⁺ concentration was obtained from the measured pH values using the correction method proposed by Irving *et al.*³² The PSEQUAD program was used to calculate the protonation and stability constants.³³

¹⁷O NMR measurements

Longitudinal and transverse ¹⁷O relaxation rates and chemical shifts were measured between 277 and 371 K. The measurements were performed using a Bruker ARX-400 (9.4 T, 54.2 MHz) spectrometer. A Bruker VT-1000 temperature control unit was used to maintain constant temperature, measured by a substitution technique. The samples were sealed in glass spheres, adapted to 10-mm NMR tubes, in order to eliminate susceptibility corrections to the chemical shifts.³⁴ A HClO₄ solution (pH = 3.0) was used as external reference. Longitudinal and transverse relaxation rates, 1/*T*₁ and 1/*T*₂, were obtained by the inversion recovery and the Carr–Purcell–Meiboom–Gill spin echo technique, respectively.

NMRD

The longitudinal ^1H relaxation rates (NMRD profiles) were obtained at 278, 298, 310, 323 K on a Stellar Spinmaster FFC fast field cycling NMR relaxometer equipped with a VTC90 temperature control unit (Stelar, Italy) ($2 \times 10^{-4} - 0.47$ T, (corresponding to a proton Larmor frequency range 0.01–20 MHz). At higher fields, the longitudinal ^1H relaxation times were measured on Bruker Minispecs mq30 (30 MHz), mq40 (40 MHz) and mq60 (60 MHz) and on Bruker 50 MHz (1.18 T), 100 MHz (2.35 T) and 200 MHz (4.70 T) cryomagnets connected to a Bruker AC-200 console. In each case, the temperature was measured by a substitution technique.

EPR

The EPR spectra were recorded on a Bruker ElexSys spectrometer E500 at X-band (9.4 GHz) (278, 298, 310 and 329 K), Q-band (34.6 GHz) (277, 299, 312 and 322 K) and a Bruker ElexSys E680 spectrometer at W-band (94.2 GHz) (286.7 K). A controlled nitrogen gas flow was used to maintain a constant temperature, measured by a substitution technique. The peak-to-peak line width was obtained from the experimental spectra using the MATLAB program.

Data analysis

The analysis of ^{17}O NMR and EPR data was performed either with a program working on a MATLAB platform version 5.3³⁵ or with Scientist[®] for Windows[™] by Micromath[®], version 2.0. The reported errors correspond to one standard deviation obtained by the statistical analysis.

Acknowledgements

We thank Dr Robert Ruloff for scientific advice. This research was financially supported by the Swiss National Science Foundation and the Office for Education and Science (OFES). This work was carried out in the frame of the EC COST Action D18 and the European-founded EMIL programme (LSHC-2004–503569).

References

- É. Tóth, L. Helm, A. E. Merbach, Relaxivity of Gadolinium(III) Complexes: Theory and Mechanism in *The Chemistry of Contrast Agents in Medical Magnetic Resonance Imaging*, ed. É. Tóth, and A. E. Merbach, Wiley, Chichester, UK, 2001, pp. 45–120.
- (a) S. Rast, A. Borel, L. Helm, E. Belorizky, P. H. Fries and A. E. Merbach, *J. Am. Chem. Soc.*, 2001, **123**, 2637; (b) S. Rast, P. H. Fries, E. Belorizky, A. Borel, L. Helm and A. E. Merbach, *J. Chem. Phys.*, 2001, **115**, 7554.
- S. M. Cohen, J. Xu, E. Radkov, K. N. Raymond, M. Botta, A. Barge and S. Aime, *Inorg. Chem.*, 2000, **39**, 5747.
- S. Aime, A. Barge, M. Botta, J. A. Howard, R. Katakay, M. P. Lowe, J. M. Moloney, D. Parker and A. S. de Sousa, *Chem. Commun.*, 1999, 1047.
- R. Ruloff, É. Tóth, R. Scopelliti, R. Tripier, H. Handle and A. E. Merbach, *Chem. Commun.*, 2002, 2630–2631.
- S. Laus, R. Ruloff, É. Tóth and A. E. Merbach, *Chem. Eur. J.*, 2003, **9**, 3555.
- S. Laus, A. Sour, R. Ruloff, É. Tóth and A. E. Merbach, *Chem. Eur. J.*, 2005, **11**, 3064.
- D. J. Sawyer and J. E. Powell, *Polyhedron*, 1989, **8**, 1425.
- V. F. Vasileva, O. Y. Lavrova, N. M. Dyatlova and V. G. Yashunskii, *Zh. Obshch. Khim.*, 1966, **36**, 674.
- G. Gonzalez, D. H. Powell, V. Tissières and A. E. Merbach, *J. Phys. Chem.*, 1994, **98**, 53.
- É. Tóth, D. Pubanz, S. Vauthey, L. Helm and A. E. Merbach, *Chem. Eur. J.*, 1996, **2**, 1607.
- IUPAC Stability Constants, Academic Software and K. J. Powell, Release 1.05*, Yorks., UK LS21 2PW, 1999.
- D. J. Sawyer, J. E. Powell and H. R. Burkholder, *J. Chromatogr.*, 1988, **455**, 193.
- Y.-M. Wang, C.-H. Lee, G.-C. Liu and R.-S. Sheu, *J. Chem. Soc., Dalton Trans.*, 1998, 4113.
- C. F. G. C. Geraldès, R. Delgado, A. M. Urbano, J. Costa, F. Jasanada and F. Nepveu, *J. Chem. Soc., Dalton Trans.*, 1995, (3), 327.
- D. A. Keire, Y. H. Jang, L. Li, S. Dasgupta, W. A. Goddard III and J. E. Shively, *Inorg. Chem.*, 2001, **40**, 4310.
- D. Felder, D. Guillon, R. Levy, A. Mathis, J. F. Nicoud, J. F. Nierengarten, J. L. Rehspringer and J. Schell, *J. Mater. Chem.*, 2000, **10**, 887.
- P. Letkeman and A. E. Martell, *Inorg. Chem.*, 1979, **18**, 1284.
- H. Imura, G. R. Choppin, W. P. Cacheris, L. A. de Learie, T. J. Dunn and D. H. White, *Inorg. Chim. Acta*, 1997, **258**, 227.
- C. F. G. C. Geraldès, A. M. Urbano, M. C. Alpoim, A. D. Sherry, K.-T. Kuan, R. Rajagopalan, F. Maton and R. N. Muller, *Magn. Reson. Imaging*, 1995, **13**, 401.
- Y.-M. Wang, C. H. Lee, G.-C. Liu and R.-S. Sheu, *J. Chem. Soc., Dalton Trans.*, 1998, 4113.
- A. Borel, L. Helm, A. E. Merbach, Molecular Dynamics of Gd(III) Complexes in Aqueous Solution by HF EPR in *Very High Frequency (VHF) ESR/EPR Biological Magnetic Resonance*, ed. L. J. Berliner, Plenum Press, NY, USA, 2004, ch. 6, vol. 22, pp. 207–247.
- L. Burai, É. Tóth, H. Bazin, M. Benmelouka, Z. Jászberényi, L. and A. E. Merbach, *Dalton Trans.*, submitted.
- D. H. Powell, O. M. Ni Dhubbghaill, D. Pubanz, L. Helm, Y. S. Lebedev, W. Schlaepfer and A. E. Merbach, *J. Am. Chem. Soc.*, 1996, **118**, 9333.
- F. Yerly, K. I. Hardcastle, L. Helm, S. Aime, M. Botta and A. E. Merbach, *Chem. Eur. J.*, 2002, **8**, 1031.
- P. Caravan, É. Tóth, A. Rockenbauer and A. E. Merbach, *J. Am. Chem. Soc.*, 1999, **121**, 10403.
- J. P. Dubost, J. M. Leger, M. H. Langlois, D. Meyer and M. Schaefer, *C. R. Acad. Sci. Paris*, 1991, **312**, 349.
- E. T. Clarke and A. E. Martell, *Inorg. Chim. Acta*, 1991, **190**, 37.
- W. P. Cacheris, S. K. Nickle and A. D. Sherry, *Inorg. Chem.*, 1987, **26**, 958.
- E. Balogh, R. Tripier, R. Ruloff and É. Tóth, *Dalton Trans.*, 2005, 1058–1065.
- S. Pavlov, M. Bogavac and V. Arsenijevic, *Bull. Soc. Chim. Fr.*, 1974, **12**, 2985.
- H. M. Irving, M. G. Miles and L. Pettit, *Anal. Chim. Acta*, 1967, **28**, 475.
- L. Zékány, I. Nagypál, in *Computation Methods for Determination of Formation Constants*, ed. D. J. Leggett, Plenum, NY, USA, 1985, p. 291.
- A. D. Hugi, L. Helm and A. E. Merbach, *Helv. Chim. Acta*, 1985, **68**, 508.
- F. Yerly, *VISUALISEUR 2.2.4. and OPTIMISEUR 2.2.4.*, 1999, Institute of Molecular and Biological Chemistry, University of Lausanne, Switzerland.